Temporal Stability of 3D-PR based on Multidimensional Golden Means: Simulation and Implementation

R. W-C. Chan[1], and D. B. Plewes[2]

[1]Department of Medical Biophysics, University of Toronto, Toronto, ON, Canada, [2]Department of Medical Imaging, Sunnybrook Health Sciences Centre, Toronto, ON, Canada

INTRODUCTION

Adaptive sampling of k-space allows images in dynamic contrast-enhanced (DCE)-MRI to be reconstructed at various spatial and temporal resolutions from the same dataset. Golden-angle radial k-space sampling achieves this flexibility in-plane with samples incremented by the golden angle, $\phi = (\sqrt{5} - 1)/2 * 180°$ [1,2]. These projections fill 2D k-space with projections that have a relatively uniform angular distribution for any time interval. We extend this method to 3D Projection Reconstruction (3D-PR) using multidimensional golden means, which are derived from modified Fibonacci sequences by an eigenvalue-eigenvector approach [3,4,5]. Successive 3D radial projections are chosen based on two ratios from the two-dimensional golden means. Conventional 3D-PR schemes restrict reconstruction to specific ***commensurate*** projection sets that form a spherically-isotropic set of radial directions in k-space. On the other hand, the golden 3D-PR approach provides a relatively uniform coverage of 3D radial k-space directions for any number of projections including ***incommensurate*** projection numbers, that, in conventional schemes, have incomplete sets of radial directions.

METHODS

Using simulations and experiments, we evaluated the *temporal jittering* (caused by undersampling artifacts) of the golden 3D-PR method and compared it to conventional 3D-PR sampling. The temporal jittering was measured as the degree of fluctuation in signal intensity, and calculated as the root-mean-square deviation from the mean signal in time.

Sampling Schemes:

i) Golden 3D-PR Sampling: The first of the higher dimensional golden means (0.4656) determined the *kz* location while the second (0.6823) determined the in-plane angle of the 3D radial projections. The k-space direction of each successive projection is unique.

ii) Conventional 3D-PR Sampling: For comparison, k-space was sampled with a conventional isotropic 3D-PR scheme that used a fixed isotropic set [6] of 1024 projections sampled repeatedly. These were divided into 4 interleaves (each having 256 isotropic projections, multiples of which correspond to the commensurate set). Projections within each interleave were acquired with linear or bit-reversed ordering.

Simulations & MRI Experiments: Phantoms were used to evaluate the temporal stability of the signal over time. In the simulations, a square object was used whose analytic k-space was sampled. In the experiments, a uniform rectangular phantom of water doped with Gd-DTPA was scanned with a fast SPGR sequence with TE/TR/flip= 3.9/11.3ms/30° and an isotropic FOV of 12x12x12cm.

Image Reconstruction: For both simulations and experiments, images were reconstructed over a range of discrete projections. The k-space data was gridded, compensated for sampling density, and a fast Fourier Transform was performed to obtain the image. The degree of temporal jittering was evaluated for a single central slice out of the 3D volume, and determined for a range of temporal/spatial resolutions. This included *commensurate* projection numbers (256, 512, 768 and 1024, which are multiples of the number of projections in an interleave) and *incommensurate* (all other) projection sets. Images from simulations and experiments were reconstructed using the same approach.

RESULTS & DISCUSSION

At commensurate reconstruction sets (as seen in Fig.1a,b at 256 projections), the conventional 3D-PR method has temporal jittering that is lower (in simulations) or comparable (in experiments) to the golden 3D-PR approach. At most incommensurate projections sets, the golden 3D-PR technique has reduced jittering (as seen in Fig.1a,b with 160 projections) and improved temporal stability compared to the conventional linear and bit-reversed methods. The temporal jittering of the bit-reversed conventional scheme and the golden 3D-PR methods approach similar values beyond 600 projections. Disparities between simulations and experiment are likely due to noise. MR images from experiments (Fig.2) illustrate the undersampling artifacts for specific cases of 256 (commensurate, Fig.2a,c,e) and 160 (incommensurate, Fig.2b,d,f) projections. The conventional techniques are best at commensurate projections when a complete isotropic set of radial directions have been sampled, but rapidly degrade when the number of projections become incommensurate with that which make up an isotropic interleave of the conventional scheme. The approximate uniformity across all projection sets (including incommensurate ones) provided by the golden 3D-PR technique allows for improved temporal stability.

CONCLUSIONS

We have demonstrated both experimentally and using simulations that the golden 3D-PR achieves higher temporal stability compared to conventional methods for most projection sets. The golden 3D-PR technique is suitable for breast DCE-MRI as it increases the flexibility of image reconstruction in a way that minimizes temporal fluctuation caused by undersampling artifacts.

REFERENCES **[1]** Winkelmann, S. IEEE Trans Med Imaging 2007;26:68-76 **[2]** Song HK, et al. Proc. ISMRM 2006, Seattle, p.3364. **[3]** Anderson PG. Applications of Fibonacci Numbers, 1993;(5):1-9. **[4]** Chan R.W., Plewes D.B. Proc. ISMRM Workshop on Non-Cartesian MRI, 2007, Sedona. **[5]** Chan R.W., Plewes D.B. Proc. ISMRM 2007, Berlin. **[6]** Wong ST, et al. MRM, 1994;32(6):778-84.

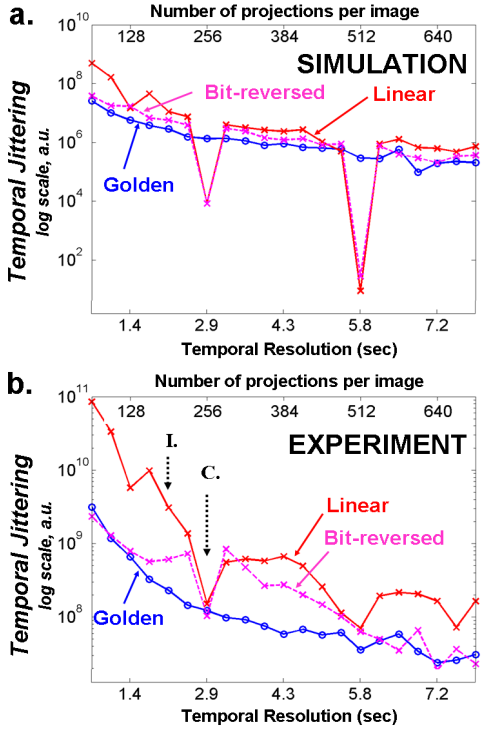

Figure 1: The temporal jittering from simulation studies **(a)** and MRI experiments **(b)** are shown for 3 sampling schemes: i) conventional 3D-PR with linear ordering, ii) conventional 3D-PR with bit-reversed order, and iii) "golden" 3D-PR derived from higher dimensional golden means. Examples of commensurate (C) and incommensurate (I) projection sets are shown.

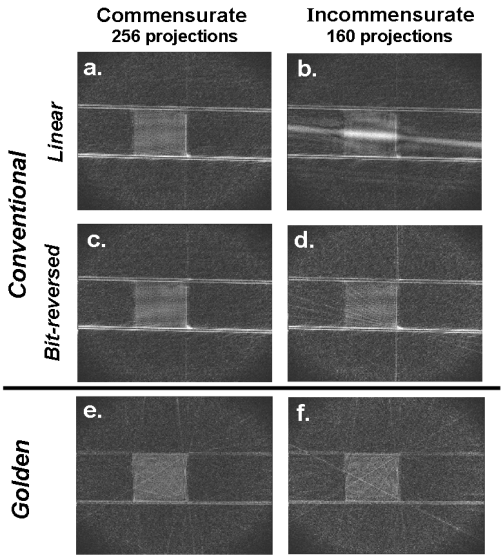

Figure 2: MR images comparing the image quality reconstructed from all three sampling schemes are shown. They are reconstructed using 256 projections **(a,c,d)** (commensurate with the number of projections in one interleave of the conventional method) and with 160 projections **(b,d,f)** (incommensurate).